Zeitschrift: IABSE reports = Rapports AIPC = IVBH Berichte
Band: 54 (1987)

Artikel: Constitutive relations for transient conditions
Autor: Wittmann, Folker H. / Roelfstra, Pieter E.
DOI: https://doi.org/10.5169/seals-41935

Constitutive Relations for Transient Conditions

Lois constitutives pour des conditions transitoires

Werkstoffgesetze unter nichtstationären Bedingungen

Folker H. WITTMANN
Professor
Swiss Fed. Inst. of Techn.
Lausanne, Switzerland

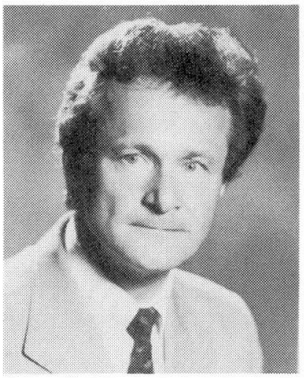

Folker H. Wittmann, born 1936, habilitated in Physics of Building Materials at Munich Institute of Technology. For 4 years he was professor for Building Materials at Delft University of Technology, The Netherlands. He is now professor and director of the Laboratory for Building Materials at the Swiss Federal Institute of Technology, Lausanne.

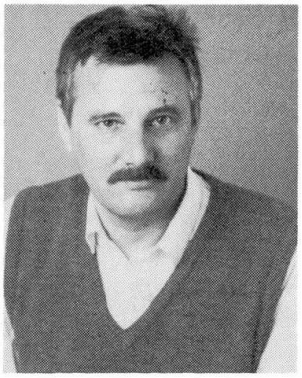

Pieter E. Roelfstra, born 1946, got his civil engineering degree at Delft University of Technology, The Netherlands. For 12 years he was involved in structural engineering at the Ministry of Public Works. Actually he is head of the group Modelling and Numerical Analysis of the Laboratory for Building Materials at the Swiss Federal Institute of Technology, Lausanne.

Pieter E. ROELFSTRA
Civil Engineer
Swiss Fed. Inst. of Techn.
Lausanne, Switzerland

SUMMARY

In order to link material properties with their structure, three structural levels are introduced. First of all, the ageing of the cement-based matrix under transient conditions is modeled. Then the time-dependent deformations of a composite material are determined by applying the concept of numerical concrete. A quasi-homogeneous material with statistically distributed properties is used to elucidate the influence of strain softening and crack formation on total deformation. Thermal incompatibility of the composite structure is taken into consideration.

RÉSUMÉ

Dans le but de lier les propriétés du matériau à sa structure, trois niveaux structuraux ont été introduits. Le vieillissement de la matrice de pâte de ciment a été introduit dans le modèle sous des conditions non stationnaires. Puis, l'application du concept du béton numérique permet de déterminer les déformations en fonction du temps d'une structure composite. Un matériau quasi-homogène avec une distribution statistique des propriétés a été utilisé pour élucider l'influence du radoucissement et de la formation de fissures sur la déformation totale. L'incompatibilité thermique de la structure composite a été prise en compte.

ZUSAMMENFASSUNG

Drei Gefügeniveaus werden definiert und eingeführt. Dann wird zunächst die Alterung der Zementsteinmatrix unter nichtstationären Bedingungen simuliert. Unter Anwendung des Konzepts 'der numerische Beton' werden die zeitabhängigen Verformungen eines zusammengesetzten Werkstoffes beschrieben. Ein quasi-homogenes Material mit statistisch verteilten Eigenschaften wurde generiert, um den Einfluss der Verformungserweichung und der Rissbildung auf die Gesamtverformung unter Beweis zu stellen. Die thermische Inkompatibilität eines zusammengesetzten Werkstoffes wird berücksichtigt.

1. INTRODUCTION

Basic creep of concrete that means creep without moisture exchange can be predicted within a reasonable confidence interval. Based on experimental results basic creep can be predicted for a wide range of different concrete compositions. A power function describes the time-dependence of basic creep sufficiently well. It is also known for a long time that creep under sealed conditions is high compared to creep of dry concrete. Many authors have even stated that creep of dry concrete can be neglected.

It is somewhat more difficult to describe shrinkage of concrete correctly. Nevertheless there are again sufficient experimental data which allow us to predict the time-dependence, the final value, and the influence of geometry reasonably well if the concrete composition and the environmental conditions are given (see for instance [1].

Controversal views still exist, however, on the most common type of time dependent deformation, i.e. simultaneous creep and shrinkage [2]. Some authors believe that creep under these conditions is magnified while others prefer to attribute the observed increase of the total deformation to an increased shrinkage. In these discussions it has not always been fully realised that simultaneous creep and shrinkage have to be considered to be a transient hygral deformation.

In most codes creep under drying conditions is indicated to be considerably bigger for all durations of load than basic creep under sealed conditions. If it is true that this time-dependent deformation is a transient process creep of a drying specimen must become negligibly small once a structural element is dried, than on the long run basic creep may become bigger.

One reason for the fact that this important aspect of concrete behaviour is still under discussion is that the different and interrelated processes are so complex that most experimental data cannot be interpreted straight away. So far numerical simulation methods are the only means to come to a better understanding. It has been outlined elsewhere in which way the concept of numerical concrete can be applied to simulate elastic deformations of a composite material and drying of a composite material with a porous matrix [3]. In this paper it is also shown that the interfacial zones have an important influence on the time-dependence of drying and on the moisture distribution within a drying specimen.

Results described in [3] will be used here as a basis for further investigations.

The major aim of this contribution is to point out that the concept of numerical concrete [4,5] can be applied to describe transient hygral deformations of a composite material such as concrete. Special emphasis will be placed on the significance of strain softening and crack formation for hygral deformations. Finally it will be shown that thermal transient conditions can be dealt with in a similar way.

2. CONSTANT AND TIME DEPENDENT STATE PARAMETERS IN THE 3L-APPROACH

2.1 General remarks

Concrete is a composite material with a porous matrix. During the hardening of the cement based matrix and before a load is applied a complex state of stresses is created in the structure due to thermal and chemical shrinkage [6]. When the formwork is removed drying of a concrete element begins. As a consequence two types of additional stresses are created : (a) tensile stresses in zones near the surface and compressive stresses in the humid center caused by the time-dependent moisture gradient, and (b) tensile stresses in the drying matrix and compressive stresses in the inert aggregates. In reality the situation is further complicated by the fact that the properties of the cement based matrix change (aging effect) as the hydration continues. In the dried outer zones, however, hydration is soon stopped. This leads to an inhomogeneous porous matrix.

It has been pointed out earlier that the structure of concrete can be subdivided at least in three different hierarchic structural levels [2]. The basic ideas of this concept, which is now called 3L- Approach, are outlined in detail elsewhere [3].

The microlevel serves to describe the processes in and the properties of the porous matrix. Advanced numerical simulation methods can be applied to introduce realistic state parameters such as degree of hydration, moisture content, moisture capacity and permeability. The mesolevel has been introduced to take the composite structure of the material into consideration. If the composite structure of concrete is simulated in a realistic way and if the point properties are sufficiently well known the response of structural elements can be predicted under arbitrary conditions.

This systematic study can be considered to be a rational way to develop material laws. The macrolevel of the 3L-Approach is finally used to formulate these relations in such a way that they can be directly applied in computerized structural analysis.

2.2 Modelling of the microstructure

2.2.1 Formation of the structure and aging

In this chapter we describe briefly new developments of modelling the formation of the microstructure of hardened cement paste with the help of numerical methods. All mechanical and physical properties of hardened cement paste are linked directly with its microstructure. Thus, if we are able to simulate the formation of the microstructure and build in real micro-mechanisms, then it is possible in principle at least to deduce constitutive relations which describe mechanical and physical behaviour of hcp under simple and very complex conditions. The first step in this direction has been done at NBS [24]. They simulated the formation of the microstructure in 3D of cement compound C_3S with a shrinkage core model and obtained in this way useful information on the pore size distribution and the contact zones between C_3S particles.

Extension of this model for different types of cement (cements having a different clinker composition) is possible if we can describe the different hydration rates of each compound and their mutual interaction in realistic way. Research on this level has therefore to be focused on reaction kinetics [7,8,9].

Terms like aging may probably be replaced in the futur by for instance contact surface between hydrating particles or time-dependent bond density [10].

For the mechanical analysis of such a simulated structure, which we might call numerical HCP, we have to investigate whether continuum or discrete mechanics is most appropriate. We should mention here also an earlier developed model from which some basic concepts can possibly be implemented [11].

2.2.2 Degree of hydration in a drying sample

The hydration process under transient conditions can be described in principle by three differential equations [25].

$$
\begin{aligned}
C_H \dot{h} + p\dot{\alpha} &= \nabla \cdot (\lambda_{HH} \nabla h + \lambda_{HT} \nabla T) \\
C_T \dot{T} - q\dot{\alpha} &= \nabla \cdot (\lambda_{TH} \nabla h + \lambda_{TT} \nabla T) \qquad (1) \\
\dot{\alpha} &= F_1(\alpha) \cdot F_2(T) \cdot F_3(h)
\end{aligned}
$$

where C_H and C_T are hygral and thermal capacities respectively, h is the relative humidity, T is the temperature, λ_{HH} and λ_{HT} are cross permeabilities and α is the degree of hydration. Coefficients p and q depend on the type of cement. This system of differential equations is highly nonlinear, because all materials properties depend strongly on actual temperature, humidity and degree of hydration. Functions $F_1(\alpha)$, $F_2(T)$ and $F_3(h)$ have to be determined from experimental results. A relatively small computer code has been developed to solve this system of equations under constant or variable boundary conditions [4]. Two typical results are shown in Figs. 1 and 2.

In Fig. 1 we can see that the degree of hydration remains low in the region near the surface which is exposed to drying. This means that mechanical properties such as modulus of elasticity, which are linked directly with the degree of hydration, vary also under these conditions as function of the distance to the surface. At the same time permeability is higher in the surface region.

Fig. 2 shows that due to self dessiccation moisture content in the center part decreases and hence moisture gradients are built up with respect to the wet boundary. These gradients cause the observed water uptake of specimen stored under these conditions.

With this model the evolution of state parameters such as temperature, humidity and degree of hydration as function of time and space can be described. This is an essential step in the so-called point property approach.

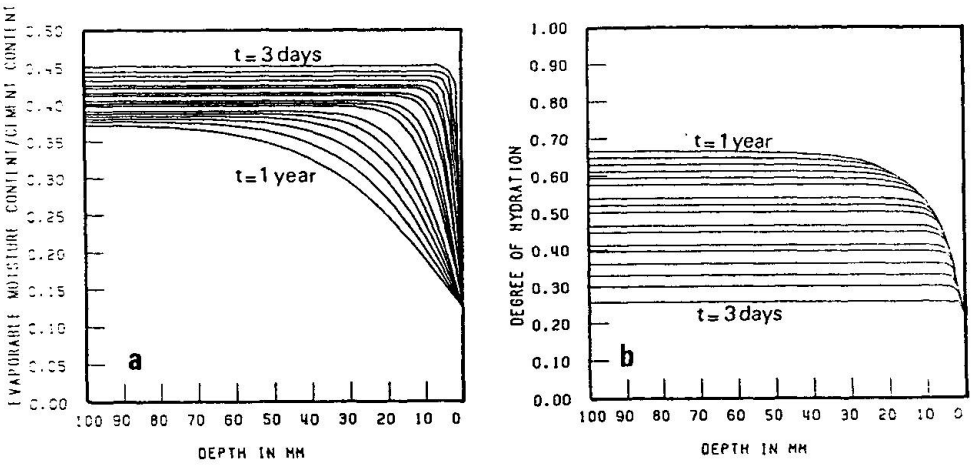

Fig. 1 Evolution of evaporable water content (a) and degree of hydration (b) as function of time and distance from the surface of a wall with a thickness of 200 mm exposed to a relative humidity of 50 %.

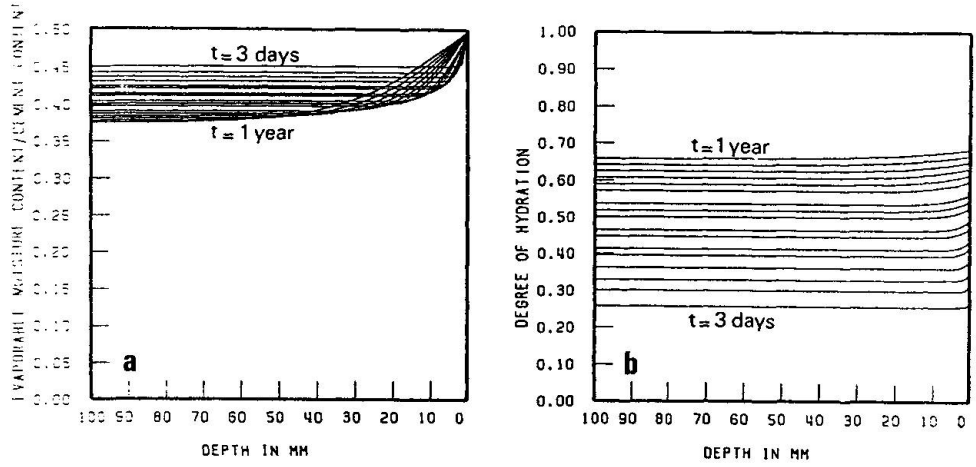

Fig. 2 Evolution of the evaporable water content (a) and degree of hydration (b) as function of time and distance from the surface of a wall with a thickness of 200 mm stored under water.

2.3 Modelling of the composite structure

Composite structures with arbitrarely shaped aggregates grains can be simulated with a computer [12]. Aggregate volume content and particle size distribution can be taken into consideration [5,13]. A typical example is shown in Fig. 3a. For the analysis the generated structure has to be idealized by a finite element mesh. It has turned out that the interface between matrix and aggregate grains with its characteristic properties has to be taken into account separately. In this contribution we used for simplicity a composite structure with 27 circular aggregate grains as shown in Fig. 3b.

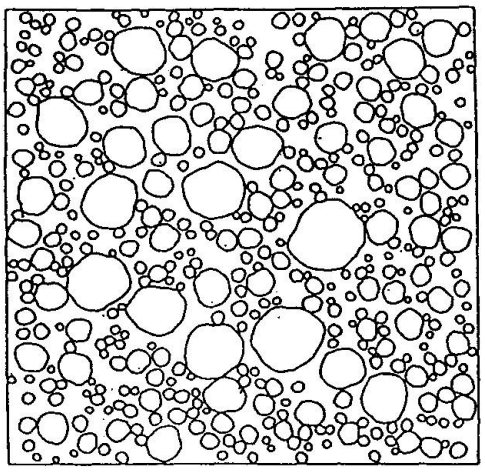

Fig. 3a Computer simulated composite structure of normal concrete.

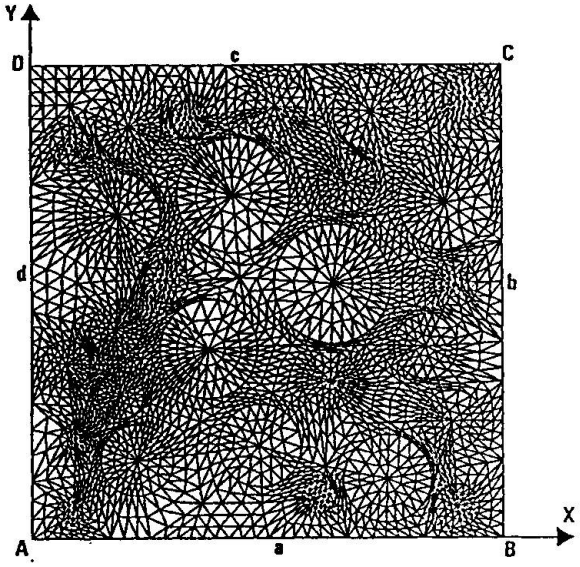

Fig. 3b Finite element idealization of the composite structure used in the analysis.

3 BASIC CREEP AND DRYING OF A COMPOSITE MATERIAL

3.1 Basic creep of a composite material

The complex state of stress in the simulated structure of concrete (see Fig. 3b) under loading conditions is shown in [3]. This structure is used here to study the time-dependent behaviour under sustained load and under isohygral conditions (basic creep). It is assumed that the aggregate grains in the structure behave perfectly linear elastic and that the small contributions of creep of the interfaces to the global (macroscopical) creep may be neglected. Due to creep the complex stress distribution in the material will change in time. The non linear rate type creep law we used for this situation is given in eq. (2) :

$$\dot{\varepsilon} = \frac{1}{m\tau_D} \frac{a_1 a_2 \sinh b\sigma}{bE}^{m} \frac{1}{\left[\int_t^t |\dot{\varepsilon}| d\tau\right]^{m-1}} \qquad (2)$$

where σ is the actual stress, $b = 1.8/fc'$ is a measure for nonlinear creep, fc' is the compressive strength, $a_1 = \exp[Q/R(1/F_0 - 1/T)]$ is Arrhenius's equation to take the influence of the actual temperature T into consideration, Q is the activation energy, R is the universal gas constant, T_0 is the reference temperature (usually $T_0 = 293^0K$), $a_2 = (12h-5)/7$ is the expression to take the influence of the actual pore humidity h into consideration (in case of basic creep a_2 is a constant), E is Young's modulus and τ_D is the time in days after loading at which the creep strain is equal to the elastic strain for $a_1 a_2 = 1$ and σ is constant. m is a positive number representing a material constant and $\left[\int_t^t |\dot{\varepsilon}| d\tau\right]$ is the actual path length of the creep strain (intrinsic time). For a constant stress, temperature and pore humidity this equation can be integrated analytically and one will find a power law according to eq. (3) :

$$\varepsilon(t-t') = \frac{t-t'}{\tau_D}^{\frac{1}{m}} \frac{a_1 a_2 \sinh(b\sigma)}{bE} \qquad (3)$$

It should be noted that eq. (2) does not take into account aging and creep recovery. Aging effects on mechanical and physical properties can be modelled by means of the concept described in chapter 2. Creep recovery needs, however, not to be modelled as a separate phenomena. The origin for creep recovery is caused by the residual potential energies in the elastic components of the composite structure after unloading and is the logic result of an appropriate analysis and application of numerical concrete.

In the example given here we used the same distribution of Young's modulus of the mortar matrix elements as described in [3]. In addition time τ_D of eq. (2) was varied according to a Gaussian distribution (τ_D = 31 days, p = 10 days, cut off at 1 and 61 days). The positive materials coefficient m has been chosen to be 3 and the product $a_1 \cdot a_2$ was fixed to be 1. The composite structure was submitted to an external compressive load of σ_y = -10 N/mm^2. Fig. 4 shows the total strain as function of duration of load (t-t'). The macro-creep strain as function of the duration (t-t') is plotted on a log-log scale in Fig. 5.

In Fig. 5 it can be seen that the "effective" basic creep strain of the composite structure describes almost perfectly a power law. The effective compliance function is given in eq. (4) :

$$\varepsilon_T(t-t') = \frac{\sigma}{E}\left[1 + \left(\frac{t-t'}{109}\right)^{0.324}\right] \qquad (4)$$

where E = 29874 N/mm^2 is the effective modulus of elasticity as calculated in [3].

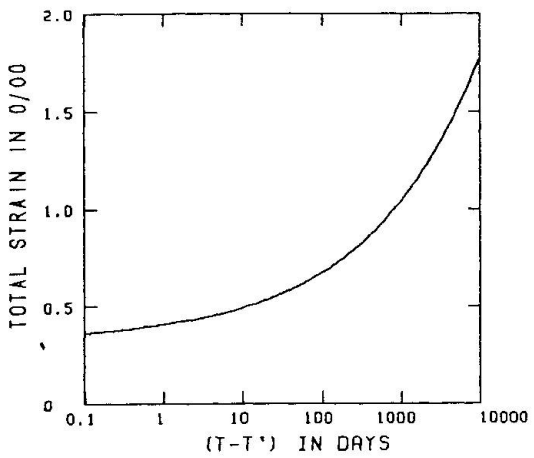

Fig. 4 Calculated total strain as function of duration of load (linear ordinate).

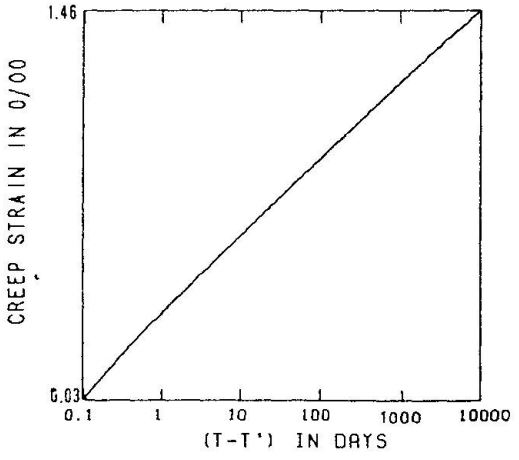

Fig. 5 Calculated basic macrocreep as function of duration of load (t-t') (logarithmic ordinate).

Fig. 6 shows the redistribution of potential energies in the different components of the composite material as function of the duration of load (t-t´).

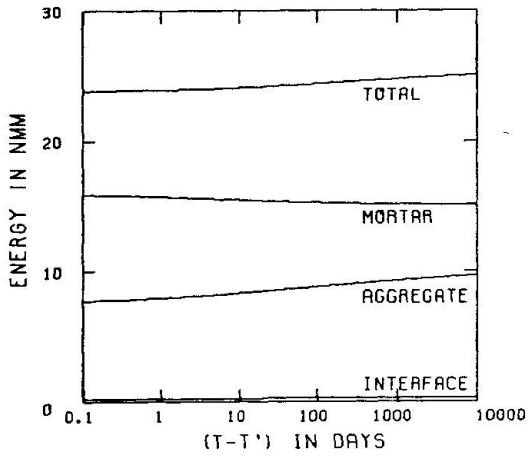

Fig. 6 Distribution of potential energies stored in the different components and the total value as function of duration of load (t-t´).

As can be seen in Fig. 6 there is a transfer from potential energy of the mortar matrix to the aggregate grains. After unloading this energy is freed again an thus this internal redistribution of energy can be considered as the driving force for partial creep recovery. The model has still to be extended with elastic components in the mortar matrix and even in HCP. From analysis performed with the extended model a generalized macro-creep law or algorithm will be deduced. It is doubtfull whether such a creep law on the macro-level can be expressed in one simple compliance function. We should mention here a mathematical expression for macro-creep strain which gives qualitatively correct deviations from the linear superposition principle [14].

3.2 Drying and hygral shrinkage of a composite material

In the point property approach we can state that hygral shrinkage depends linearly on pore humidity h. The real mechanisms of hygral shrinkage such as change of surface energy and disjoining pressure with changing pore humidity are explained elsewhere [15]. This implies that in principle the overall shrinkage of a composite structure can be determined if the evolution of the distribution of the pore humidity as function of time can be calculated. Simulation of the drying process of a composite material is carried out in [3].

In Fig. 7 the calculated moisture distribution of a composite material, 3 days after exposing to drying, is shown.

Assuming that the unrestrained hygral shrinkage of the mortar matrix is linked to pore humidity h linearly as indicated by eq. (5) and using the initial strain concept in the numerical analysis, the overall (macro) shrinkage can be determined.

$$\varepsilon_{us} = -0.002 + 0.00002\ h \quad (h \text{ in } \%) \tag{5}$$

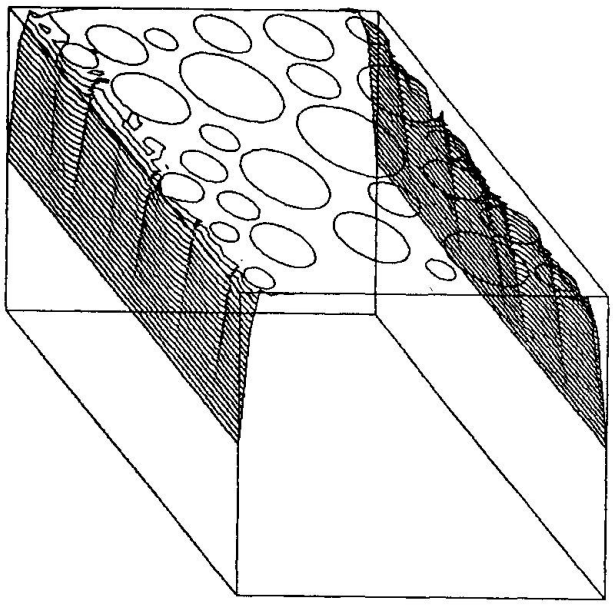

Fig. 7 Calculated moisture distribution of a composite material 3 days after exposing to drying (see [3].)

The deformations of the composite structure calculated in this way are shown in Fig. 8.

In Fig. 9 the corresponding major stress distribution in the mortar matrix is shown. In this figure the length of the lines is a measure for the major stress level. From the analysis of the tensile major stresses (max. ~14 N/mm^2) it becomes obvious that without taking crack formation into consideration no realistic result could be obtained. In earlier codes of numerical concrete we had already introduced crack formation with a tensile strain softening concept [5,16]. In these codes the direction of the softening behaviour was fixed in the elements at the moment the major stress exceeded the tensile strength. The direction of the major stress in the next loading steps, however, did not always coincide with the fixed direction of softening. This is caused by redistributions in the very complex state of stresses of the composite material. Consequently, some elements kept a certain rigidity in the major stress direction and were "locked". This problem can possibly be overcome by using a multiple crack model. In this context we should mention here a very attractive mathematical framework which can handle multiple crack formation without violation material frame indifference [17]. The implementation of such a model in the numerical concrete codes will, however, increases computer time considerably because one needs to keep track of the state of every crack. Another solution is the use of an isotropic strain softening model which can be justified on grounds of the relative small mesh sizes which are used in the numerical concrete structures [4].

A concept which is certainly more satisfying from a materials science point of view is the prediction of multiaxial softening relations by simulating crack formation and propagation in mortar structures with LEFM [18,19]. It is essential that these models take care of friction. Further studies are needed to find out which solution is the most realistic and convenient one. Therefore, the influence of crack formation on shrinkage is first studied by means of a simplified model which will be discussed in the next paragraph.

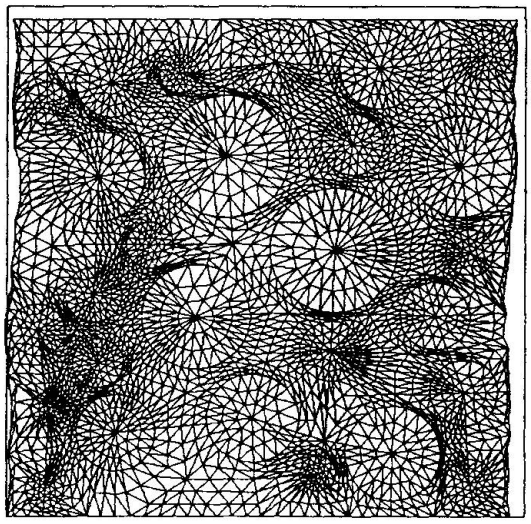

Fig. 8 Calculated deformations corresponding to the stage of drying shown in Fig. 7.

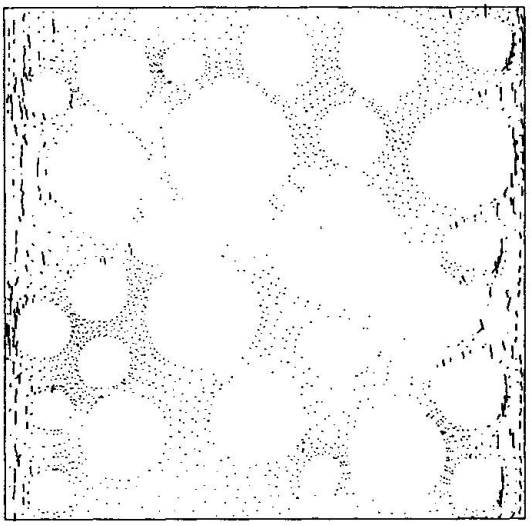

Fig. 9 Calculated major stress distribution in the mortar matrix corresponding to the stage of drying shown in Fig.7.

4 DEFORMATION UNDER TRANSIENT HYGRAL CONDITIONS

4.1 Numerical model of a quasi homogeneous material

It has been shown in the preceeding chapter how the drying of a composite structure can be predicted numerically. We have seen that the resulting stresses in the material overcome tensile strength of the matrix. As has been pointed out finally crack formation in the composite structure will be taken into consideration. For the moment being we will use a numerical model of a quasi homogeneous material to investigate the effect of crack formation on the total deformation under transient hygral conditions.

A computer code has been developed to predict the time dependent behaviour of concrete slabs [4]. The length and the thickness of the slab can be introduced. For the analysis a regular mesh with simple triangular finite elements is generated automatically. Coarser and finer meshes can be chosen by the user.

It is assumed that the drying process takes place perpendicular to the two parallel and opposite surfaces of the slab. The nonlinear drying process can therefore be calculated uniaxially, and all nodes with the same distance to the surface have the same time dependent humidity.

Creep and shrinkage have been introduced in a similar way as described in the preceeding paragraphs. In addition a strain-hardening and softening model has been introduced. To simulate the localization processes in regions with high tensile stresses a statistical distribution of the tensile strength has been assumed. Details of this model are described elsewhere [4,26]. The strain-hardening and softening model used in the following two examples is shown in Fig. 10.

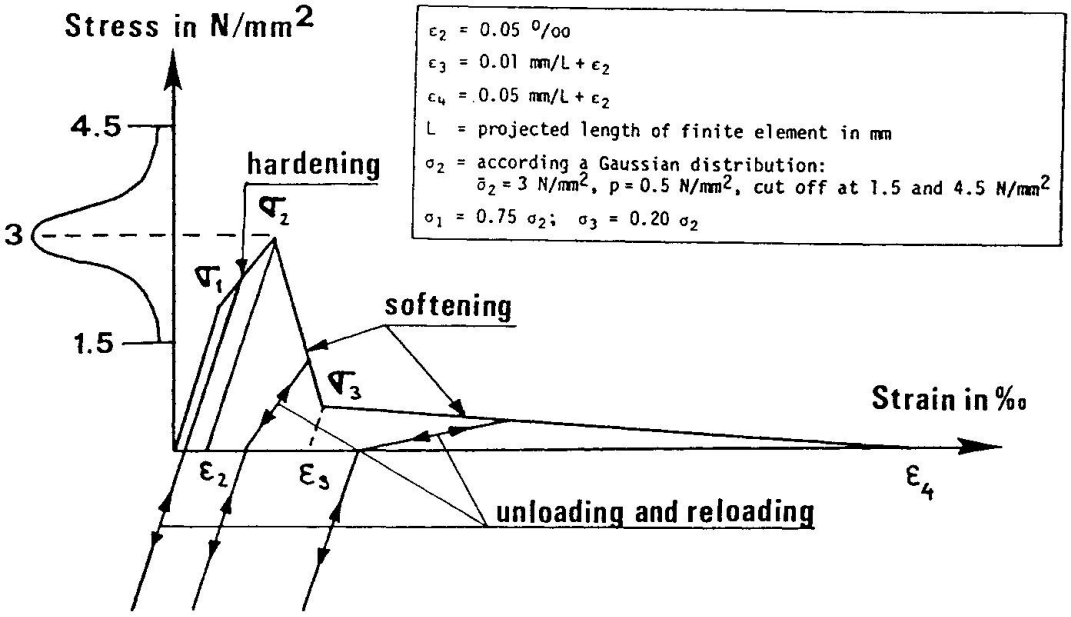

Fig. 10 Strain-hardening and softening model applied in the analyses.

4.2 Influence of crack formation on total deformation under hygral transient conditions

As an example we will simulate shrinkage of a slab of a thickness of 120 mm and a height of 240 mm. The slab is supposed to be exposed at both sides to air with a relative humidity of 50 %. The unrestrained shrinkage is supposed to be :

$$\varepsilon_{us} = -0.0018 + 0.000018\ h \quad (h \text{ in } \%) \qquad (6)$$

At 50 % RH this corresponds to a final shrinkage deformation of -0.9 o/oo.

First the uniaxial distribution of humidity as function of time was calculated with the nonlinear diffusion equation described elsewhere [20].

In Fig. 11 the calculated deformations, the distribution of damage energy and the zones where strain softening occurs (localization process) after three different durations of drying are shown.

In this model we call damage energy the amount of energy which is consumed in the tensile strain hardening branch of the diagram shown in Fig. 10. It should be noted that in this analysis tensile strain hardening and softening behaviour was fixed in advance in the longitudinal direction of the slab to gain CPU time. As can be seen in Fig. 11 localization of strain softening has taken place in 3 regions, but a complete stress-free crack was not created. This is due to tensile creep behaviour and the assumed distribution of the tensile strength. In this model the influence of tensile creep on strain softening is not yet taken into account explicitely. This is a subject which needs to be developed further in order to simulate realistically subcritical loading conditions.

The calculated shrinkage curve (a) of the slab is shown in Fig. 12.

As can be seen the final shrinkage of curve a is lower than the assumed unrestrained shrinkage of -0.9 o/oo corresponding to a relative humidity of 50 %. This is caused by the residual strain in the softening regions after unloading (see fig. 10 and fig. 11). Curve b in Fig. 12 represents the calculated shrinkage curve for which hardening and softening behaviour was suppressed by increasing the tensile strength. This curve can be considered to be the shrinkage curve under compressive loading conditions. The final shrinkage of this curve is higher than the unrestrained shrinkage at 50 % RH. This is caused by the influence of humidity on the creep rate. During the drying process tensile creep takes place in the dry regions, while compressive creep takes place in the wetter core. Thus, although the internal stress field (caused by drying) is in equilibrium, the overall (macroscopic) creep is not zero and increases shrinkage without crack formation. In Fig. 13 the ratio between curve (b) and curve (a) as function of duration of drying ($t-t'$) is shown. From this analysis it can be concluded that there is a marked difference between shrinkage under load and free shrinkage reduced by crack formation (which is the shrinkage we generally measure in our experiments). This difference will probably still be increased if we take the heterogeneous structure of concrete into consideration.

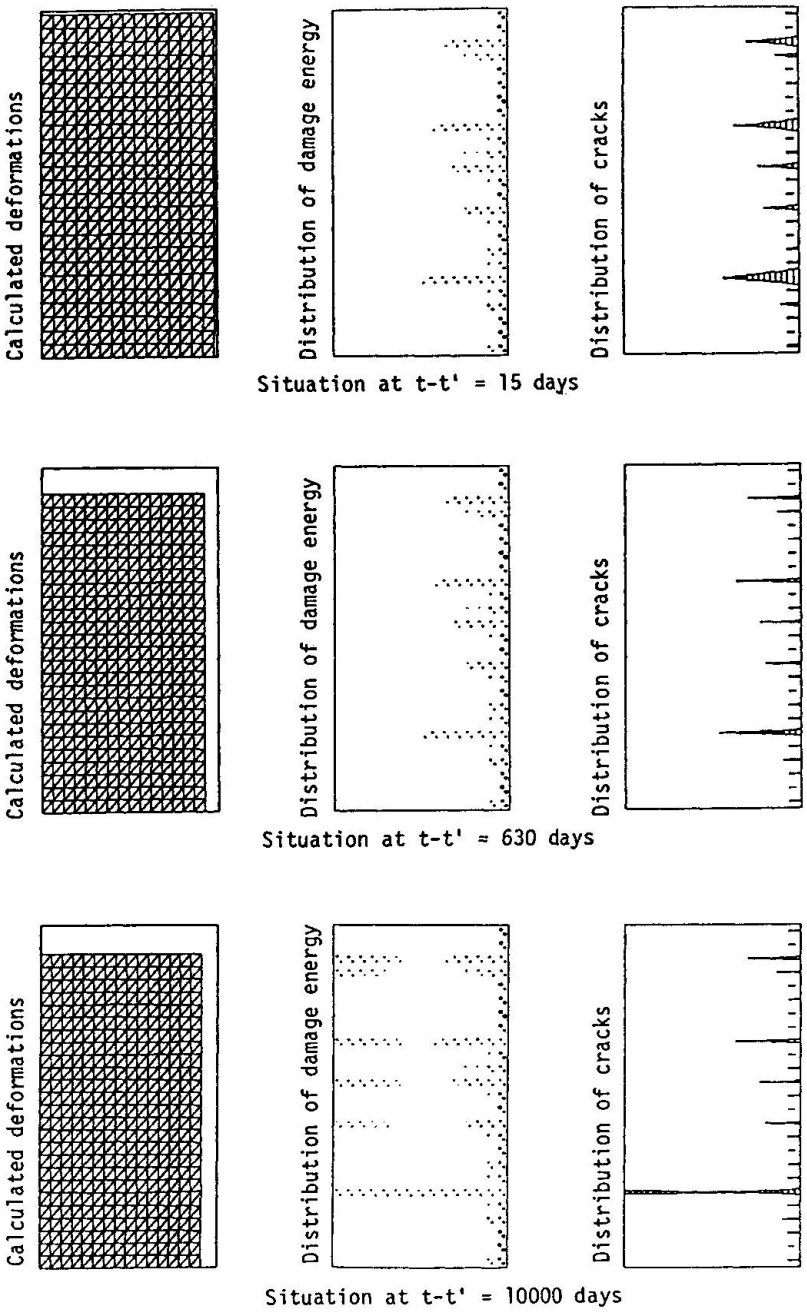

Fig. 11 Calculated deformations, distributions of damage energy and strain softening at three different durations of drying.

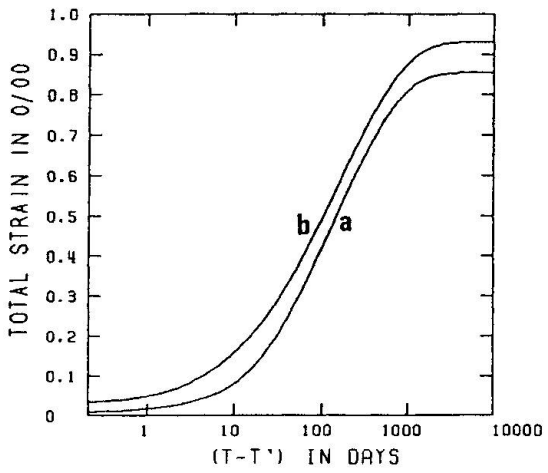

Fig. 12 Calculated shrinkage curves with (a) and without (b) crack formation as function of duration of drying.

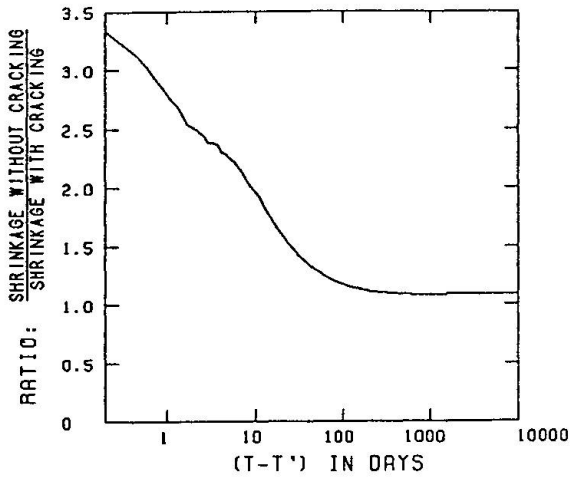

Fig. 13 Ratio of shrinkage without and shrinkage with crack formation as function of duration of drying.

In Fig. 14 experimental results of creep and shrinkage tests on sealed and drying cylinders of HCP are shown [21]. When we determine again the ratio between the shrinkage under load ε_s and the free shrinkage ε_s^o we obtain the curves shown in Fig. 15. The applied load is indicated as parameter.

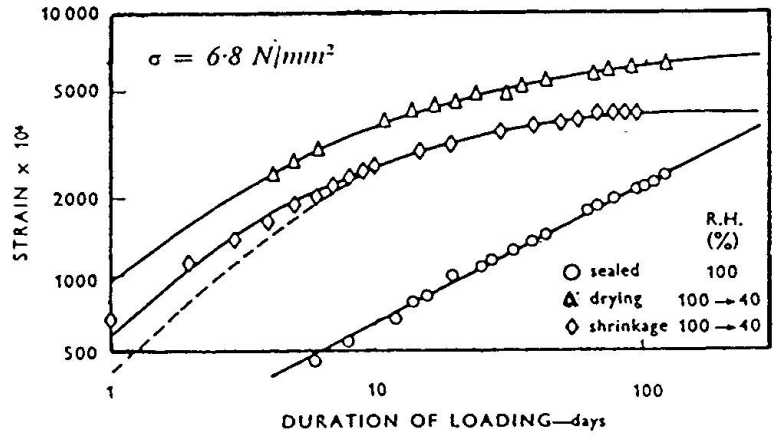

Fig. 14 Creep of hollow cylinders of HCP. Results of tests carried out under sealed conditions (at 100 % RH) and under drying conditions (from 100 % to 40 % RH). Pure shrinkage is also shown [21].

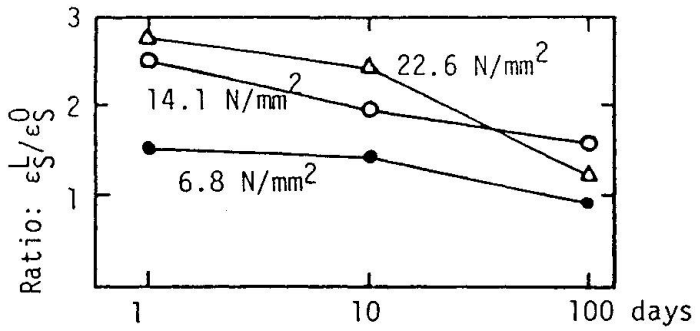

Fig. 15 Ratio between shrinkage under loading ε_s^L and free shrinkage ε_s^0 as function of duration of drying. Applied external stress is the parameter. (Data after [21]).

A number of results of similar test series has been evaluated in the same way. At the beginning always a factor of about 2 or slightly bigger has been found and as drying proceeds this factor decreases and approaches finally 1. The relation shown in Fig. 15 agrees qualitatively well with the numerical prediction shown in Fig. 13. This relation can be considered to be characteristic for transient hygral deformation. For longer periods of drying the remaining creep function corresponds to the lower creep of dried concrete. The result of this analysis may still be modified once the circumferential stresses around the aggregates are taken into consideration.

The model has further been used to study geometrical effects on shrinkage. In our laboratory very accurate shrinkage measurements have been carried out on cylinders with different diameters [1]. These cylinders were exposed to a relative humidity of the surrounding air of 65 %. In Fig. 16 the measured shrinkage strains at different durations of drying are indicated.

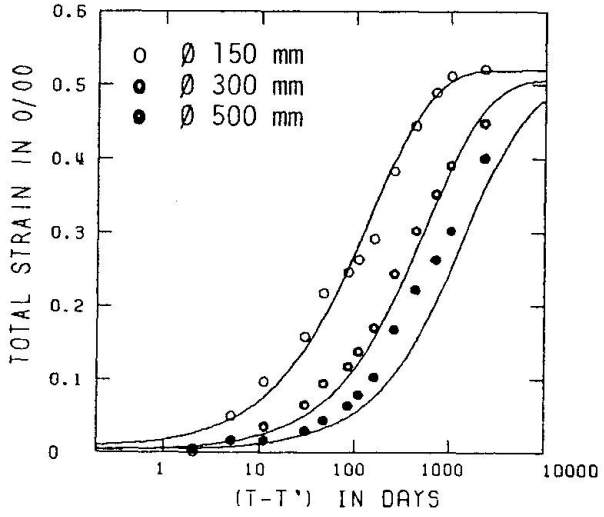

Fig. 16 Comparison between measured shrinkage strains of cylinders with Ø 150 mm 300 mm and 500 mm, exposed to RH 65 %, and calculated shrinkage curves based on a nonlinear diffusion equation and a tensile strain-hardening and softening model with residual strains. Measurements by [1].

In the model moisture capacities, permeabilities and unrestrained shrinkage were adopted to get a close fit with the shrinkage measurements of the cylinder with a diameter of 150 mm. Next the same materials data were used to predict the shrinkage curves of the cylinders with diameters 300 mm and 500 mm. Results are shown also in Fig. 16. It should be noted that we used "equivalent" thickness of the slabs calculated with the model in order to be able to compare with the results obtained experimentally with cylinders. As can be seen in Fig. 16, the predicted final shrinkage with the model becomes less as the geometry increases. This corresponds well with the results just mentioned [1] as well as with other experimental findings [22].

Although generally a reasonable agreement between experimental results shown in Fig. 16 and the numerical prediction can be observed there remains a systematic deviation. The shrinkage prediction based on diffusion theory underestimates the hygral deformation at longer durations of drying and for bigger specimens. This discrepancy can be explained by the fact that aging of the material is not represented adequately in the model. Aging can have different effects on shrinkage. The diffusion coefficient decreases, the final value of shrinkage can even increase due to the presence of more hydration products and finally the increased tensile strength leads to an accelerated shrinkage due to reduced crack formation.

5 DEFORMATION UNDER TRANSIENT THERMAL CONDITIONS

5.1 Influence of a sudden change of temperature on basic creep of a composite material

It has been shown above that drying creates a complex state of stress in a composite material (see Fig. 9). In case the coefficients of thermal dilatation of the matrix and the aggregates are not identical any temperature change necessarely must create internal stresses. In Fig. 17 a typical example of a numerical simulation of this situation is shown [13]. In this case α_M for the matrix has been chosen to be $12 \cdot 10^{-6}$ K^{-1} and α_A for the aggregates has been chosen to be $7 \cdot 10^{-6}$ K^{-1}. The tensile stresses in the aggregates and the compressive stresses in the matrix are indicated by means of their major stresses.

Now let us suppose that the composite structure shown in Fig. 3b is loaded at room temperature and the creep is measured until $t-t' = 15$ days. Then the temperature is linearly increased to 70^0C in 12 hours and the resulting deformations are further followed.

This situation has been simulated numerically and results are shown in Fig. 18. During the initial period modest basic creep is observed. When the temperature is changed first of all a thermal expansion is noticed and later the thermally increased basic creep follows. In the left part of Fig. 18 the elastic energy of the different components is plotted. The aggregates are temporarely partly unloaded while the surrounding matrix has to take over the corresponding compressive stresses. Due to the increased creep at elevated temperatures these stresses are quickly reduced.

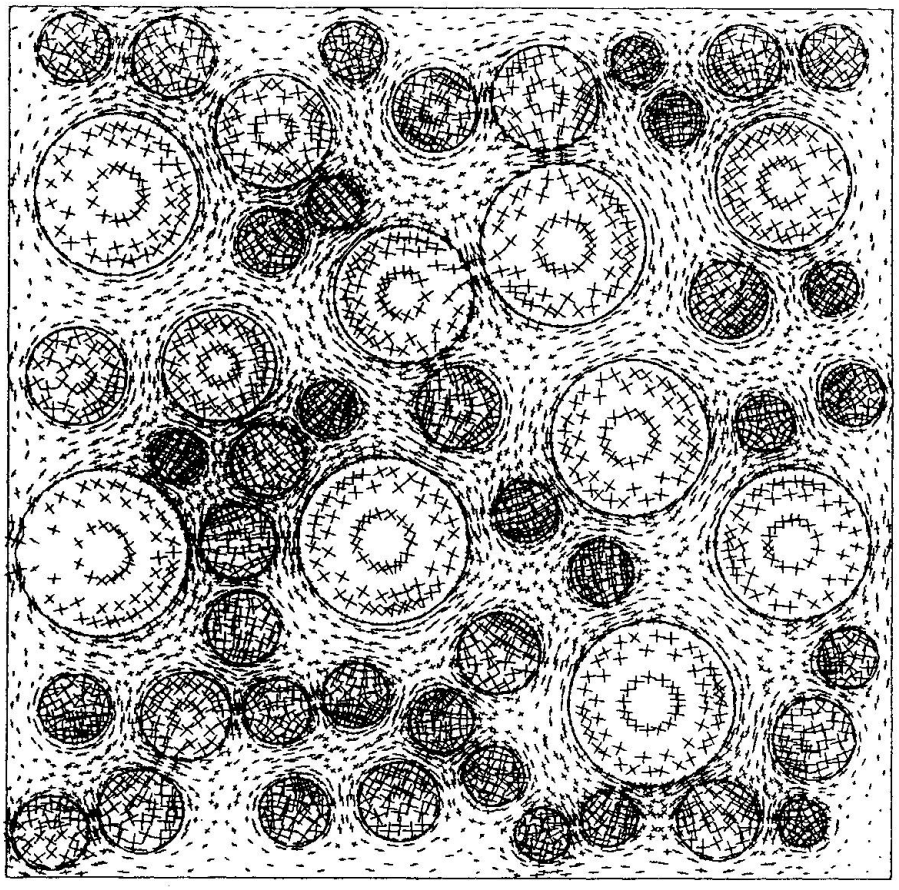

Fig. 17 Calculated major stress distribution in a composite structure due to a thermal shock.

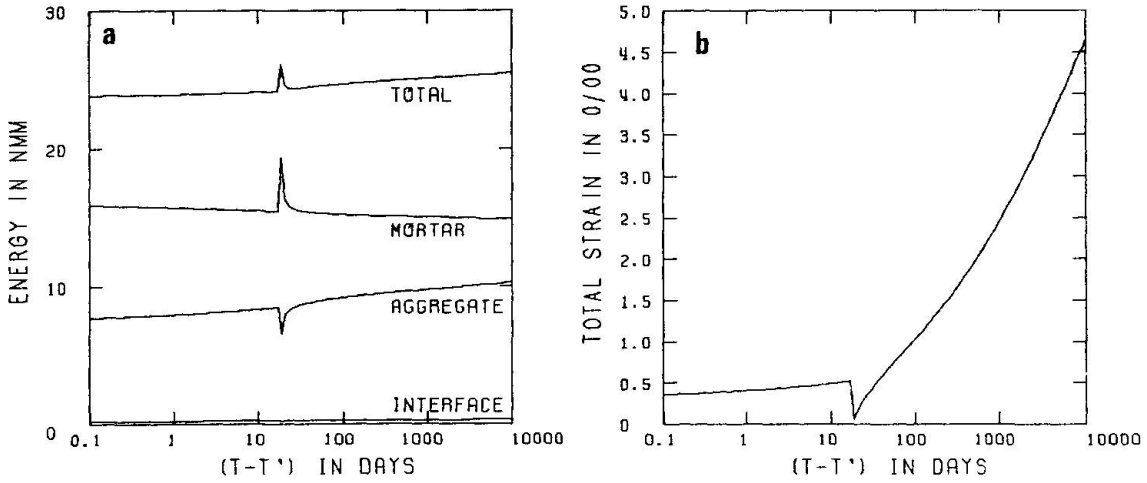

Fig. 18 (a) Distribution of potential energies stored in the components and total stored potential energy as functionof duration of loading.
(b) Total deformation as function of duration of loading.
The temperature is kept constant at 20^0C up to (t-t´) = 15 days; then the temperature is linearly increased in 12 hours to 70^0C and further kept constant.

5.2 Influence of sudden change of temperature on drying and total deformation

In the preceeding section we have supposed that the specimen was tested under sealed conditions. Let us now repeat the theoretical experiment of 5.1 but this time under drying condition, i.e. in 50 % RH.

In Fig. 19 the loss of evaporable water is plotted as function of time. For comparison the drying under isothermal conditions (20^0C) are shown too. For further details of this calculation we refer to [3,23]. In this same publication the influence of temperature on the water capacity and the permeability are given. At $t-t' = 15$ days the drying rate increases noticebly.

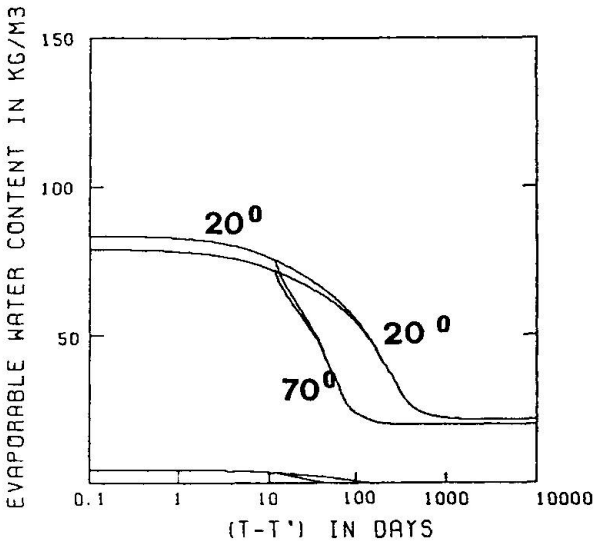

Fig. 19 Loss of evaporable water as function of duration of drying for two different temperature histories (see also [20,23]).

The corresponding total deformation is shown in Fig. 20. Initially the time-dependent deformation is bigger because the specimen is stored in a drying environment. The change of temperature cause first of all again thermal expansion. Then the creep at elevated temperatures sets in at an increased rate. The drying process and hence shrinkage comes to an end at about 200 days. Then creep rate must be expected to be considerably slowed down.

For comparison the total time-dependent deformations shown in Figs 19 and 20 are replotted in Fig. 21. The initial increase of deformation under drying conditions can clearly be seen. While the sealed sample continues to creep at a high rate after the temperature change the drying sample undergoes a transition which leads to a significantly reduced total deformation.

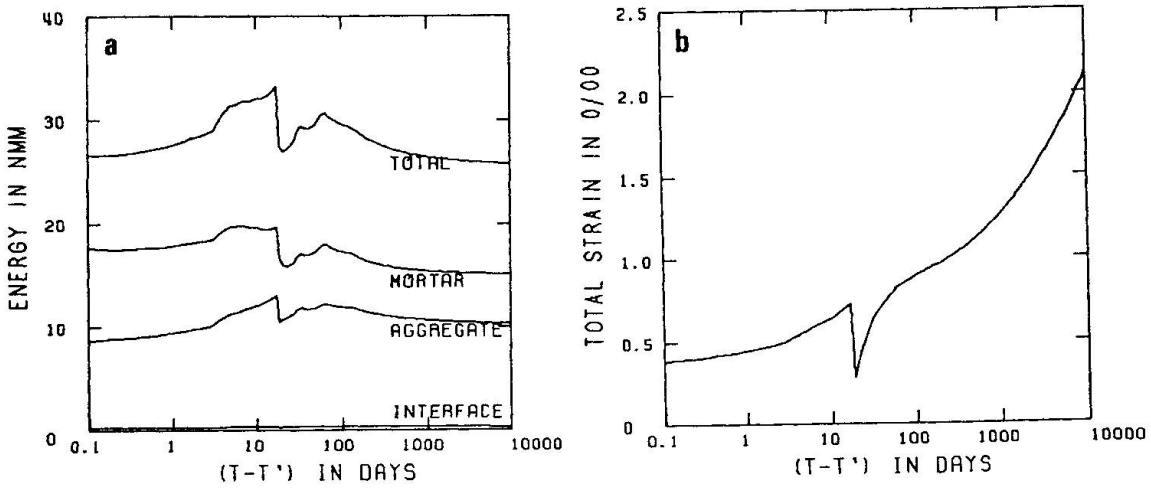

Fig. 20 (a) Distribution of potential energies stored in the components and total stored potential energy as function of duration of loading.
(b) Total deformation as function of duration of loading.
The drying process starts at the moment the load is applied.
The temperature is kept constant at 20^0C up to (t-t') = 15 days; then the temperature is linearly increased in 12 hours to 70^0C and further kept constant.

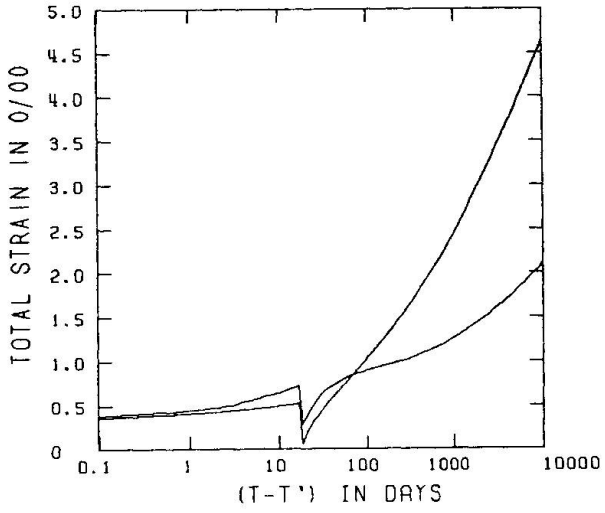

Fig. 21 Comparison between the calculated total deformations shown in Fig. 18b and Fig. 20b.

It should be noted here that the increased temperature only accelerates the transition. Under normal temperatures the same behaviour will be observed at much longer times. Further the attention is drawn to the fact that any temperature change immediately causes an increased rate of deformation due to the internal stress concentration.

6. CONCLUSIONS

- Some basic concepts of numerical simulation of the formation of the microstructure of HCP are outlined. The aim of this approach is to replace arbitrary terms like aging by more realistic terms like bond density in the xerogel and bonds between hydrating particles of HCP.
- Actual state parameters such as temperature, humidity and degree of hydration can be determined under transient hygral and thermal conditions by solving numerically a series of appropriate coupled differential equations with given boundary conditions.
- Shrinkage of a composite structure without crack formation, based on calculated moisture distributions, has been determined with numerical concrete codes.
- The influence of crack formation, tensile strain-hardening and softening on the total deformation of a quasi-homogeneous drying material has been studied by means of model based on FEM. With this model the difference between shrinkage without crack formation and shrinkage with crack formation can be quantified.
- As has been shown already earlier drying shrinkage and creep of concrete cannot be separated. The total deformation depends on thesuperimposed stress fields.
- Transient hygral deformation can be realistically predicted if the concept of point properties is applied rigorously.
- Transient thermal deformation has to be dealt with in the same way.

REFERENCES

1. ALOU F., FERRARIS C.F. and WITTMANN F.H., Etude expérimentale du retrait du béton, Mat. et Constr. RILEM (to be published 1987).
2. WITTMANN F.H., Structure and mechanical properties of concrete, The Architectural Reports of the Tohoku University, 22 (1983) pp. 93-112.
3. WITTMANN F.H. and ROELFSTRA P.E., Numerical concrete applied to predict constitutive laws of porous composite materials, SMIRT-9, Lausanne, H 2/1, (to be published 1987).
4. ROELFSTRA P.E., Numerical concrete, Ph.D. Thesis, Swiss Federal Institute of Technology, Lausanne, (to be published 1987).
5. SADOUKI H., Simulation et analyse numérique du comportement mécanique de structures composites, Ph.D. Thesis, Swiss Federal Institute of Technology, Lausanne (to be published 1987).
6. ACKER P., BOULAY C. and ROSSI P., On the importance of initial stresses in concrete and of the resulting mechanical effects, Cem. Concr. Res. (to be published 1987).
7. KNUDSEN T., On particle size distribution in cement hydration, Proc. 7th Int. Congr. Chem. Cement, Paris, Vol. II, I, (1980) pp. 170-175.
8. BEZJAK A., JELENIC I., MIAKAR V. and PANOVIC A., A kinetic study of alite hydration, Proc. 7th Int. Congr. Chem. Cement, Paris, Vol. II, I, (1980) pp. 111-116.

9. JAWED I., SKALNY J. and YOUNG J.F., Hydration of portland cement, Chapter 6 in Structure and Performance of Cements, ed. P. Barnes, Applied Science Publishers Ltd, Barking, Essex, England (1983).

10. DOUGILL J.W., Comment in Recorders Report of session 2 of the fourth RILEM International Symposium on Creep and Shrinkage of Concrete : Mathematical Modeling, held at Northwestern University, Evanston, Illinois, August 1986 (to be published 1987).

11. BAZANT Z.P., Viscoelasticity of solidifying porous material concrete, J. Eng. Mech. Div., ASCE, Vol. 103, No EM6 (1977) pp. 1049-1067.

12. WITTMANN F.H., ROELFSTRA P.E. and SADOUKI H., Simulation and analysis of composite structures, Mat. Sci. and Eng. 68 (1984-1985) pp. 239-248.

13. ROELFSTRA P.E., SADOUKI H. and WITTMANN F.H., Le béton numérique, Mat. et Constr. 107 (1985).

14. BAZANT Z.P. and TSUBAKI T., Weakly singular integral for creep rate of concrete, Mech. Res. Commun. 7 (1980) pp. 335-340.

15. WITTMANN F.H., Creep and shrinkage mechanisms, Chapter 6 in Creep and Shrinkage in Concrete Structures, Ed. by Z.P. Bazant and F.H. Wittmann, John Wiley & Sons Ltd (1982).

16. ROELFSTRA P.E. and SADOUKI H., Total fracture energy in composite materials, SVMT/DVM, Basel (1986).

17. DE-BORST, Nonlinear analysis of frictional materials, Ph.D. Thesis, Delft University of Technology, The Netherlands (1986).

18. ZAITSEV Y.U. and WITTMANN F.H., Crack propagation in a two-phase material such as concrete, Proc. 4th Int. Conf. on Fracture (ICF-4), Waterloo, Canada, Vol. 3 (1977) pp. 1197-1204.

19. HU X.Z., COTTERELL B. and MAI Y.M., Computer simulation models of fracture in concrete, In Fracture Toughness and Fracture Energy of Concrete, ed. by F.H. Wittmann, Elsevier Science Publishers, Amsterdam, The Netherlands (1986).

20. KAMP C.L., ROELFSTRA P.E. and WITTMANN F.H., Mechanisms of moisture transfer through porous materials, SMIRT-9, Lausanne (to be published 1987).

21. WITTMANN F.H. and LUKAS J., The application of rate theory to time-dependent deformation of concrete, Mag. of Concr. Res. Vol. 26, 89 (1974) pp.191-197.

22. HANSEN T.C. and MATTOCK A.H., Influence of size and shape of member on the shrinkage and creep of concrete, J. Am. Concr. Inst. 63 (1966) pp. 267-290.

23. KAMP C.L., ROELFSTRA P.E., MIHASHI H. and WITTMANN F.H., Diffusion mechanisms and drying of concrete at elevated temperatures, SMIRT-9, Lausanne (to be published 1987).

24. JENNINGS H.M. and JOHNSON S.K., Simulation of microstructural development during the hydration of a cement compound, J. Am. Ceram. Soc., 69 (1986) pp. 790-795.

25. JONASSON J.E., Moisture fixation and moisture transfer in concrete, SMIRT-8, Brussels, H5/11 (1985) pp. 235-242.

26. ROELFSTRA P.E. and WITTMANN F.H., Numerical modelling of fracture of concrete, SMIRT-9, Lausanne (to be published 1987).

Leere Seite
Blank page
Page vide